CHAPTER 3

Pluronic mediated copper nanoparticles for antimicrobial applications: Investigating the role of Pluronic concentration

3.1: Introduction

Nowadays, nanoparticles are being employed in a variety of domains such as biology, physics, chemistry, engineering, and so on [1, 2]. The key benefit of nanoparticles is that their characteristics differ significantly from those of bulk materials of similar composition. Nanoparticles' properties can easily be modified by altering their shape, size, and chemical conditions [3]. Nanoparticles, especially metal nanoparticles (MNPs), have been getting a lot of attention from scientists because they can be used in a lot of different ways, from catalysis to nanofluids, to thermal conductors to optical compounds, and magnetic devices to environmental remediation [4-6].

When compared to metallic gold and silver nanoparticles, copper's natural abundance, inexpensive, and multiple practical and easy ways of synthesizing Cu-based nanoparticles, as well as their economic viability, make CuNPs especially attractive. Micro emulsion, thermal decomposition, vapour decomposition, sol-gel, precipitation, laser ablation, electrochemical, electrospinning, aqueous chemical reduction, and microwave-assisted techniques have already been reported as physical and chemical ways for the synthesis of CuNPs [7-14]. CuNPs can be used in many different ways because of their unique chemical and physical properties [15,16]. CuNPs have been extensively applied as trace elements, fungicides, algaecides, insecticides, and herbicides in agriculture, as well as disinfectants in animal husbandry [17]. Many reviews have been reported on the synthetic pathways of CuNPs and their various newer applications, reporting optimal features such as good electrical conductivity [18], lubricating thermal [19], and excellent antimicrobial activities [20]. Because of their large surface area-to-volume ratio (SA:V) and crystalline structure, CuNPs have been shown to have a better antimicrobial effect than typical copper salts [21]. CuNPs show potent antifungal and inhibitory activities against a wide range of fungi [22-24]. The use of CuNPs is restricted due to Cu's high sensitivity to oxidation. Hence, fabricating pure and stable CuNPs is quite a difficult task. Many efforts have been made to develop synthesis paths and help materials that improve the stability of CuNPs through modifying their sensitivity towards water, chemical entities, and oxygen [25-27]. To avoid oxidation, the reactions were carried out in an inert atmosphere employing reducing agents and capping agents for the reduction of copper salt [28-30]. In the chemical reduction method, the reduction of metal ions to zero-valent metal has been done with conventional, costly, and

hazardous reducing agents. To keep away the toxic reaction, we have used Vitamin C (ascorbic acid) as a reducing agent, which also behave as a protecting agent to terminate the oxidation reaction [31]. The task of synthesizing CuNPs with significant biological effects and better media stability is clearly essential. The nanoparticles that are in a colloidal solution are very different from those that are in a biological media. When nanoparticles are placed into such biological medium, they are likely to undergo chemical and physical changes that diminish, if not eliminate, its effects. Natural and synthetic polymers or proteins are used to cap or encapsulate nanoparticles in order to make them more stable when chemical and physical changes happen in the environment [32]. They typically serve two functions: (i) to stabilize nanoparticles and build them resistant to physicochemical changes in the media in which they are present, and (ii) to fabricate nanoparticles more body-friendly, minimizing their hazardous influence on the human body and allowing them to travel through the organism's barriers unhindered. One such polymer is Pluronic. The amphiphilic POE-POP-POE tri-block copolymers can aggregate into nano micellar structure to create a variety of morphological structures. Pluronic is very appropriate for biomedical applications like drug delivery, gene therapy, and tissue engineering since it exhibits thermo reversible micellization around body temperature [33]. The main uses of Pluronic are its high biocompatibility, low biological accumulation, and microbial-film anti-adherence property, which expand its application in the area of nanomaterials [34-37]. Considering the interesting biological properties already exhibited, here we focused on the synthesis of Pluronic mediated CuNPs and the investigation of their antimicrobial efficiency. We are investigating the effect of Pluronic concentration on the synthesis and physicochemical properties of CuNPs in order to improve their versatility in the diagnosis and treatment of many diseases or microbes [38]. The organization of this work is as follows: The first was that we optimized the molar ratio of ascorbic acid to copper salt for the synthesis of CuNPs. Secondly, the CuNPs were synthesized using an optimized ascorbic acid reductant and in the presence of different-different concentrations of Pluronic F127. The synthesized Pluronic F127 mediated CuNPs have been characterized using UV-Vis spectroscopy, DLS, Zeta potential, XRD, FE-SEM, and EDX measurements. The antibacterial activities of F127 mediated CuNPs were examined against Gram-negative bacteria like *Escherichia coli* (*E. coli*) and *Pseudomonas aeruginosa* (*P. aeruginosa*), and Gram-positive

bacteria like *Staphylococcus aureus* (*S. aureus*) and *Bacillus subtilis* (*B. subtilis*), and the antifungal activities against *Fusarium oxysporum* (*F. oxysporum*), *Penicillium*, *Aspergillus niger* (*A. niger*) and *Saccharomyces cereviciae* (*S. cereviceae*).

3.2: Experimental section

3.2.1: Synthesis of CuNPs

The CuNPs were synthesized by the reduction of $CuSO_4 \cdot 5H_2O$ using ascorbic acid. Here, a typical 100 mL of 0.1 M copper sulphate pentahydrate solution was prepared in a 250 mL round-bottom flask (three necked) furnished with an oil bath and thermometer. The content was stirred and kept at 85°C for 2.5 h. A 60 mL solution of various concentrations of ascorbic acid (to maintain the ascorbic acid:Cu^{+2} salt molar ratios of 5:1, 10:1, 15:1, 20:1, and 25:1, respectively) was also prepared and added drop by drop to the copper solution with fine stirring. Meanwhile, the 1 M sodium hydroxide solution was added for neutralization in the mixture at the same temperature. The colour of the solution turned yellow after 5 min, and it was stirred for another 10 min to get the red ochre. The colloidal solutions of CuNPs were then analyzed for optimization of the reducing agent and other required experiments. The CuNPs solution was cooled, centrifuged at 8000 rpm for 15 min, filtered, washed with ultrapure water, and also with ethanol. Finally, the CuNPs were dried in a vacuum oven at 90 °C for 1 h.

3.2.2: Synthesis of Pluronic F127 mediated CuNPs

In the synthesis procedure of Pluronic F127 mediated CuNPs through the chemical reduction method represented in Figure 3.1(a), 0.1 M copper sulfate pentahydrate in different concentrations of F127 solution were taken in a round bottom flask (three-necked) and heated at 85 °C for 2.5 h with constant stirring in an oil bath. The solution changes its colour from a very light sky blue to an intense sky blue. Then, the drop-by-drop addition of 1.5 M ascorbic acid solution into the reaction mixture with vigorous stirring changed the colour of the solution to reddish-brown. The mixture was then treated with 1 M of sodium hydroxide for neutralization and kept at 85 °C. The colour of the solution turned yellow after 5 min, and it was stirred for another 10 min to get the colloidal dispersion with red ochre, which indicates the formation of CuNPs. For the solid F127 mediated CuNPs, the dispersion was cooled at room temperature (28 ± 0.5 °C) and centrifuged at 8000 rpm for 15 min. The settled CuNPs were collected and washed with ultrapure water and ethanol. The collected solid CuNPs were properly dried in a vacuum oven at 90 °C. The step-to-step colour changes that occurred in the synthesis are shown in Figure 3.1(b).

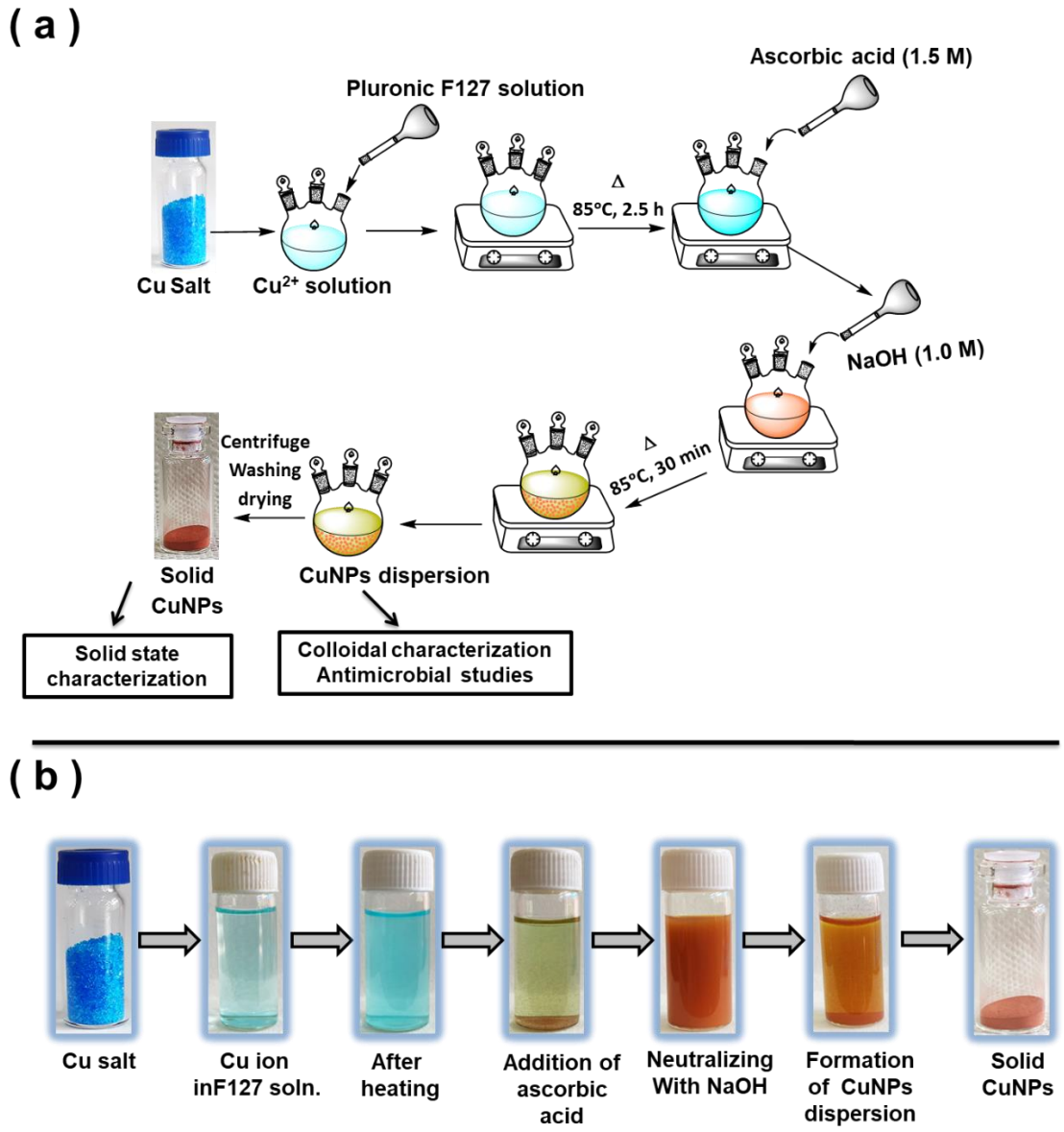

Figure 3.1: (a) Schematic representation of the synthesis of F127 mediated CuNPs using chemical reduction method. (b) Step-by-step changes of colour during the synthesis of F127 mediated CuNPs.

3.2.3: In-vitro antimicrobial activity study

In vitro antimicrobial assays were performed using the good diffusion technique [39]. The colloidal solutions of blank and Pluronic F127 mediated CuNPs were poured (100 µL) into wells bored from sterile nutrient agar plates that had previously been seeded with Gram-negative (*E. coli* and *P. aeruginosa*) bacterial cells, as well as Gram-positive (*S. aureus* and *B. subtilis*) bacterial cells. For the antifungal study, *Penicillium*, *A. niger*, *S. cerevisiae*, and *F. oxysporum*

were examined. Microbes were cultured in the well-sterile nutrient agar also with potato dextrose agar mediums. To prepare plates of nutrient agar, 28 g of the nutrient agar was compounded in 1000 mL of hot ultrapure water and mixed well upto complete dissolution. The agar solutions were sterilized for 15 min at 121°C using an autoclave and maintaining 15 lb pressure. After the agar solutions cooled down to 45°C, the ~20 mL of them were poured into sterile petri-dishes and kept for solidification. Then, after the microbes were spread on the surface of the nutrient agar using a sterile cotton swab and kept to solidify. The disc utilized in this technique had a diameter of 7-mm (~30 µg sample). After that, the wells were filled with the solution, 50µL each, in the petri-dishes cultured with the under-investigation microbes. After allowing the diffusion of blank CuNPs and F127 mediated CuNPs for 2 h, the agar plates were incubated at 37°± 0.5°C for almost 24 h for antibacterial studies, and the other prepared plates were incubated for 5 days at 25°±2°C for antifungal studies. The antimicrobial properties were determined by measuring the inhibition zone every side of each well and disc using a vernier caliper. The whole process was performed in a laminar flow chamber, except the incubation [40, 41]. Each experiment was done three times, and the mean diameters of the zones were recorded.

3.3: Results and discussion

Optimization of the reducing agent First, we prepared CuNPs in water by reducing an aqueous solution of Cu^{2+} salt with ascorbic acid as a reducing agent and sodium hydroxide to neutralize the solution by heating it at 85°C. The formation of CuNPs was confirmed by the change of solution colour from light sky blue to red ochre (see Figure 3.1(b)). In general, the molar ratio of ascorbic acid to Cu^{2+} salt has strongly impacted on the formation, particle size, and efficiency of CuNPs. Figure 3.2 shows the UV-Visible absorbance and fluorescence emission spectrums of CuNPs were produced at varied molar ratios of reactants. The CuNPs, which were prepared at a different molar ratio of ascorbic acid to Cu^{2+} salt of 5:1, 10:1, 15:1, 20:1, and 25:1, display intensity peaks in the UV-Vis spectra that are near the wavelength of 573 nm. Furthermore, a highly intense peak is absorbed when the molar ratio of ascorbic acid and Cu^{2+} salt is 15:1, which indicates the optimized reactant ratio for the formation of CuNPs. With a rise in ascorbic acid concentration, the rate of chemical reduction rises, resulting in the rapid formation of a greater number of copper nuclei and the formation of very small CuNPs, leading to enhanced aggregation of copper atoms and particles. While the ascorbic acid molar ratio was higher than 15, the absorption peaks were shown to demonstrate a decrease in intensity. Hence, results clearly showed that the ascorbic acid:Cu^{2+} salt molar ratio of 15:1 was found to be better for the synthesis of CuNPs at neutral pH, a temperature of 85°C, and a 3 h time period. Such observations were verified through the fluorescence emission spectra of the CuNPs with various molar ratios of ascorbic acid and Cu^{2+} salt (5:1, 10:1, 15:1, 20:1, and 25:1). When the ascorbic acid:Cu^{2+} salt molar ratio was set at 15:1, the CuNPs had the most fluorescence. Biocompatible Pluronic have been widely used for the straight-forward utilization of metal nanoparticles without the requirement for any purification step [39, 40]. A Pluronic polymer F127, was added to the surface of the CuNPs to make them more stable and prevent them from aggregation in biological environments, as well as to build them more biocompatible and reduce the toxicity and immune response normally induced by their interaction with living entities. Therefore, we explored the F127 polymer as the stabilizer in the CuNPs synthesis.

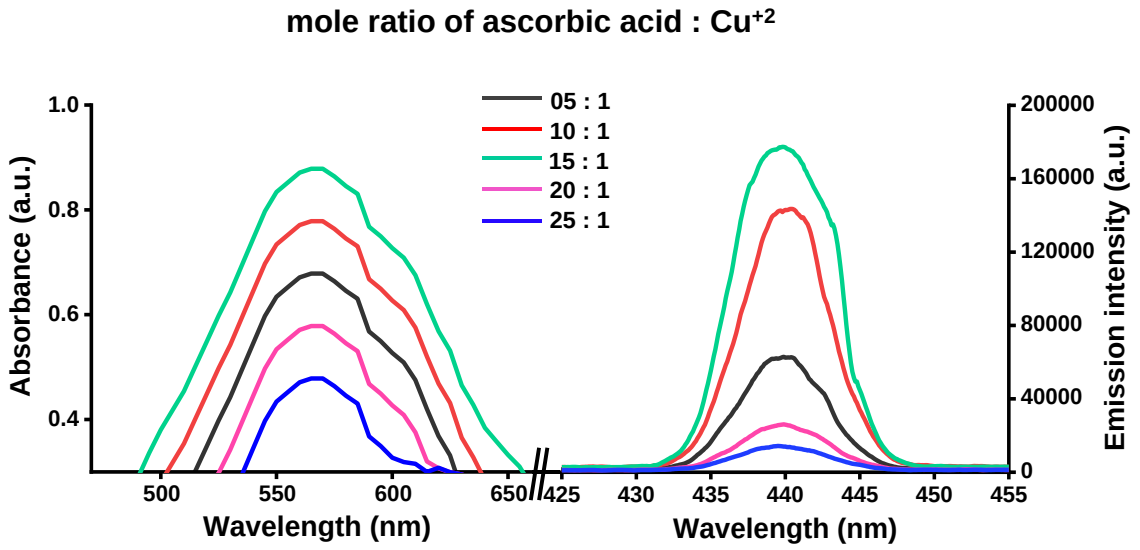

Figure 3.2: UV-Visible absorbance and steady state fluorescence spectrums of the CuNPs synthesized at various molar ratios of reactants.

3.3.1: Characterization of colloidal Pluronic F127 mediated CuNPs solution

3.3.1.1: UV-Visible spectral analysis

As shown in Figure 3.1, we synthesized Pluronic F127 mediated CuNPs under optimized conditions of 15:1 ascorbic acid-to-Cu^{2+} salt molar ratio, 85°C temperature, and neutral pH in the presence of different concentrations of F127 polymer in aqueous media. Figure 3.3 shows the optical absorbance of prepared CuNPs and F127 mediated CuNPs with different F127 polymer concentrations. The formation of CuNPs is evidenced by the appearance of the absorbance peak, which appears at 570-575 nm. The SPR showed the intensity increased with an increase in the concentration of F127 polymer. Since the position of SPR refers to different factors such as the size and shape of nanoparticles, the similar absorption peak ranges from 570-575 nm indicates that most of the CuNPs obtained had similar size and shape, and the F127 concentration did not much alter the size and shape of particles. It was clear that F127 helped to keep CuNPs stable by preventing them from aggregating [41].

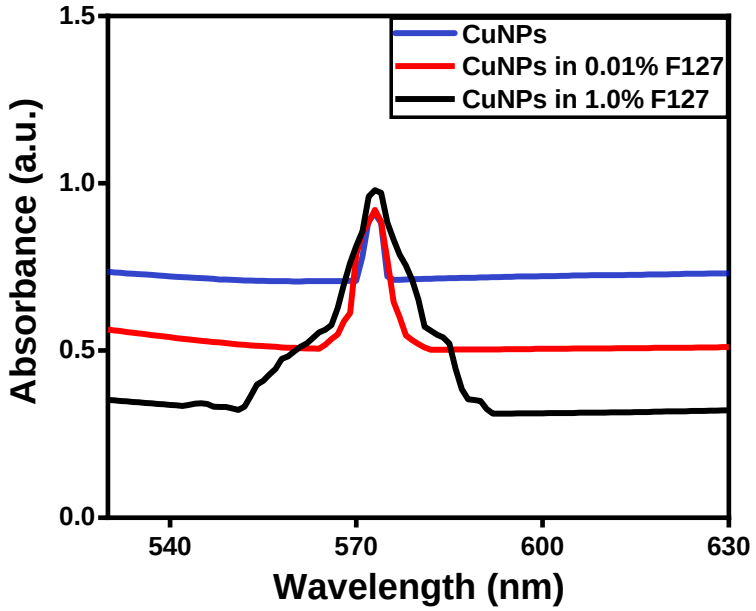

Figure 3.3: UV-Visible absorbance spectrums of the blank and F127 mediated CuNPs.

3.3.1.2: Analysis of DLS and Zeta potential

The particle size, in the form of the average hydrodynamic diameter (D_h) of CuNPs and F127 mediated CuNPs, is measured using the DLS technique. Size distribution curves of various CuNPs are shown in Figure 3.4. The D_h values of blank CuNPs, CuNPs in 0.01% F127 and CuNPs in 1.0% F127 were 45.68 nm, 43.24 nm and 38.12 nm, respectively (see Table 3.1). The particle size of F127 mediated CuNPs was found to be very much smaller than unprotected CuNPs. Results clearly indicated that with an increase in the concentration of F127 from 0.01% to 1.0%, the large CuNPs convert into the smaller CuNPs. To understand the effectiveness of surface covering by F127 at various concentrations, the zeta potential of the CuNPs colloidal solutions was monitored. Without the F127 polymer, the zeta potential of unprotected CuNPs shows a single peak at -33.50 mV (see Figure 3.5), which can be marked to the negative ascorbate ions on the CuNPs surfaces. F127 mediated CuNPs had zeta potential values of -17.28 mV and -11.10 mV, respectively. In the presence of F127, the zeta potential value has decreased from -33.50 mV to -11.10 mV, suggesting that the surface of the CuNPs has been covered with the polymer. The results also confirmed that the higher amount of F127 polymer showed better stabilization of the CuNPs in the water [42].

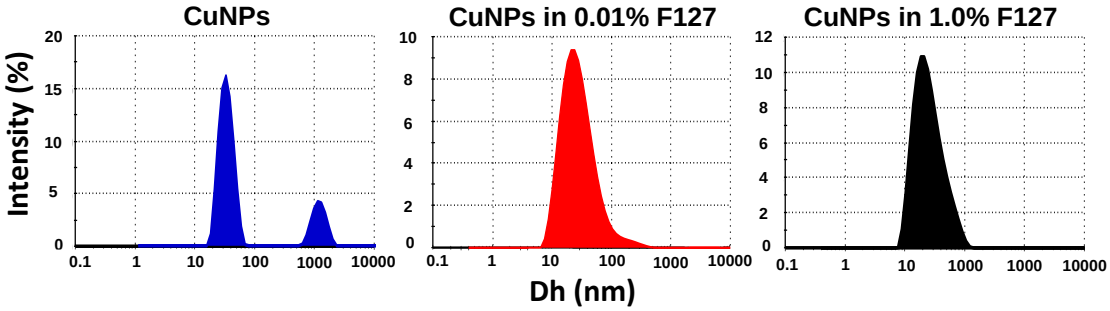

Figure 3.4: Size distribution curve of the blank and F127 mediated CuNPs at RT.

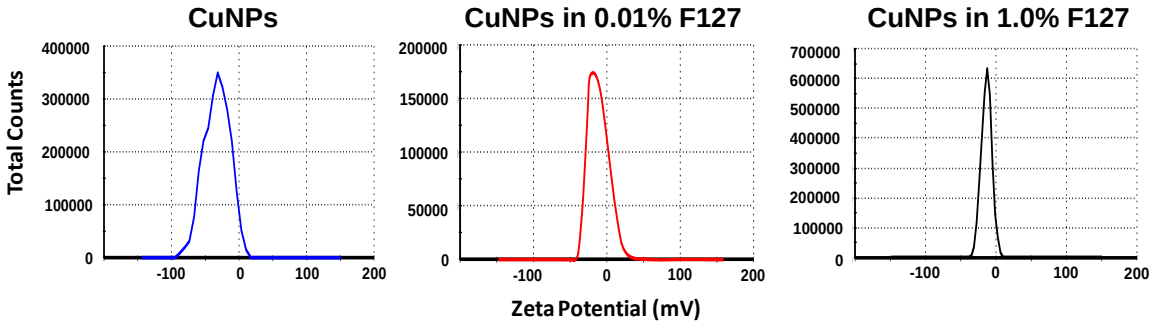

Figure 3.5: Zeta potential profile of the blank and F127 mediated CuNPs at RT.

Table 3.1: Hydrodynamic diameter (D_h) and Zeta potential values of F127 mediated CuNPs

Nanoparticles	D_h (nm)	Zeta potential (mV)
CuNPs	45.68	-33.50
CuNPs in 0.01% F127	43.24	-17.28
CuNPs in 1.0 %w/v F127	38.12	-11.10

3.3.2: Solid state characterization of F127 mediated CuNPs

3.3.2.1:X-ray diffraction analysis

The phase structure, crystallinity, and size of the CuNPs were verified by the XRD analysis. Before the XRD characterization, the F127 mediated CuNPs were centrifuged, filtered, washed with ultrapure water as well as ethanol, and dried in an oven to obtain solid state nanoparticles. Figure 3.6 shows the XRD patterns of blank CuNPs and F127 mediated CuNPs. The blank CuNPs observed the intense peaks at 2θ values of 43.42°, 50.56°, and 74.25°, which are similar to (111), (200), and (220) lattice planes, revealing the presence of pure metallic nano copper. The intense peaks of F127 mediated CuNPs found the peak at 2θ values of 43.39°, 50.53°, and

74.21°, which are similar to (111), (200), and (220) lattice planes, respectively. The X-ray pattern of all the synthesized CuNPs matched the fcc (face-centred cubic) structure of the bulk copper and its highly crystalline nature. As per the clear observations from Figure 3.6, the additional peaks were not observed in the CuNPs, indicating the absence of any CuO or Cu_2O in the synthesized nano copper. We also calculated the mean size of the CuNPs from the diffraction peaks using the Scherrer formula. The mean particle size of blank CuNPs, CuNPs in 0.01% F127, and CuNPs in 1.0% F127 was 34.53 nm, 34.02 nm, and 31.07 nm, respectively (see Table 3.2). Similar to the DLS analysis, the XRD results showed that increasing the concentration of F127 from 0.01% to 1.0% reduced the particle size of CuNPs. The obtained results understandably demonstrate that the copper ions have been reduced to nano copper with better stabilization of F127 under reaction conditions.

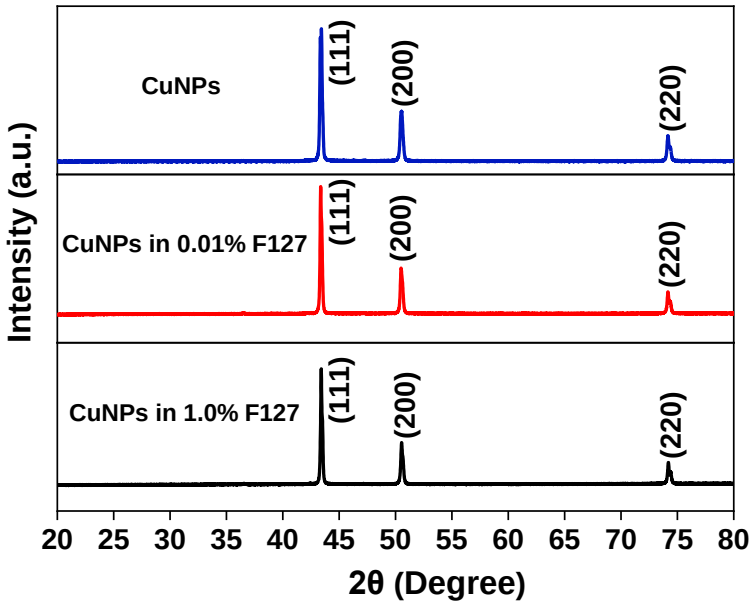

Figure 3.6: X-ray diffraction patterns of the blank and F127 mediated CuNPs.

Table 3.2: Obtained parameters of XRD and EDX analysis of the F127 mediated CuNPs.

Nanoparticles	Particlesize(nm)	Lattice constant (a Å)	Crystal structure	Elemental analysis (%w/w)	
				Copper	Carbon
CuNPs	34.53	3.608	fcc	87.66%	12.34%
CuNPs in 0.01% F127	34.02	3.610	fcc	94.39%	5.61%
CuNPs in 1.0% F127	31.06	3.610	fcc	93.50%	6.50%

3.3.2.2: FE-SEM and EDX analysis

Figure 3.7 shows the FE-SEM images of CuNPs formed by chemical reduction through ascorbic acid in an aqueous solution using increasing concentrations of F127. In the absence of F127, large CuNPs were seen in fcc-shaped and agglomerated forms. On the other hand, the addition of 0.01% F127 to the reaction yielded fcc shaped CuNPs with a smaller crystallite size. Further, when the amount of F127 was increased to 1.0%, very smaller Cu nanoparticles of the same size were seen. It indicates that the presence of F127 on the surface of CuNPs shows steric hindrance among nanoparticles, effectively preventing the aggregation. The EDX spectrum of all the synthesized CuNPs and F127 mediated CuNPs are shown in Figure 3.8. EDX analysis showed a very homogenous copper-rich composition for all the synthesized CuNPs with a purity of more than 90% copper composition. No elemental oxygen was found, eliminating the presence of oxides of copper. EDX analysis has confirmed that the CuNPs are not impure by their oxides, which are generally found in wet-chemical techniques performed in air and the alkaline environment [43].

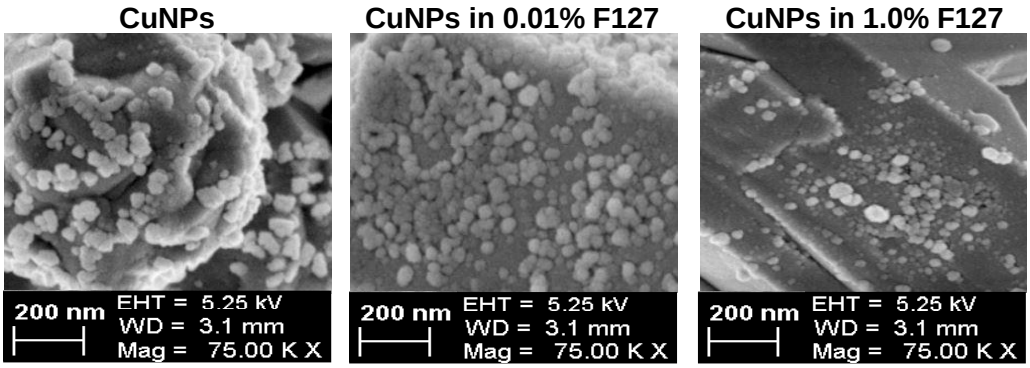

Figure 3.7: FE-SEM images of the blank and F127 mediated CuNPs.

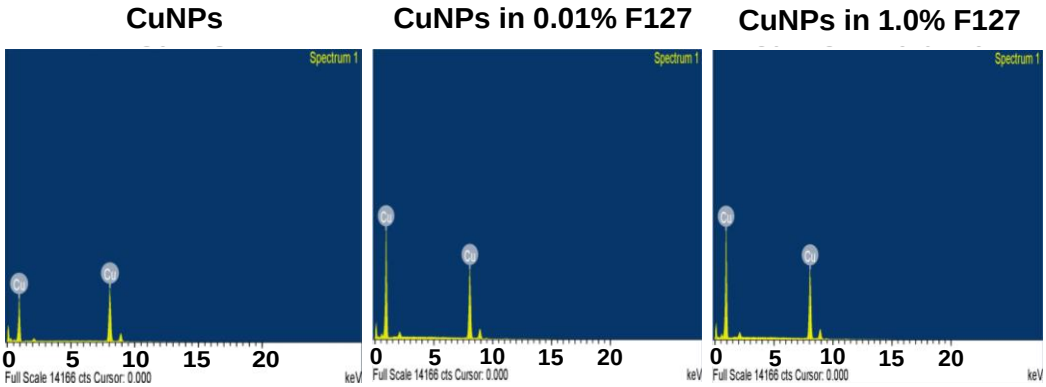

Figure 3.8: EDX spectral images of the blank and F127 mediated CuNPs.

3.3.3: Antimicrobial activity of Pluronic F127 mediated CuNPs

The antimicrobial effect of the CuNPs was evaluated with the slandered technique through the comparison of the inhibition zones created on all sides of the well where the nanoparticle samples were placed. Experiments carried out with the Pluronic F127 without CuNPs displayed no inhibition zone, which indicated that the F127 did not have any bacterial or antifungal activity in contrast to other analogous systems [44].

3.3.3.1: Antibacterial activity

The F127 mediated CuNPs in a colloidal solution were tested for their antibacterial abilities against as Gram-negative (*E. coli* and *P. areruginosa*) cells, as well as Gram-positive (*S. aureus* and *B. subtilis*) bacterial cells. The F127 content was 0.01%, 0.1%, and 1.0% in the final colloidal solution of CuNPs. Figure 3.9 shows the inhibition zones developed by the colloidal solutions of CuNPs and F127 mediated CuNPs. According to the reports, reducing the size of the metal nanoparticles enhances the interaction with bacteria and passes through the membrane with better penetration. This happens due to better diffusion of particles [45]. We expected that the F127 mediated CuNPs samples would present the larger inhibition zones with a higher F127 concentration as these nanoparticle samples possessed small particle sizes, as seen by DLS and XRD analysis. The growth inhibition of all the studied bacteria showed an increase in order due to the smaller particle sizes of F127 mediated CuNPs (from 45.68 nm to 38.12 nm as per DLS data). As seen in Table 3.3, all the F127 mediated CuNPs produced a significantly larger inhibition zone in compared to blank CuNPs. It indicated that the antibacterial activity of the nanoparticles is strongly correlated to its diffusion in the agar medium. The findings clearly demonstrated that better interaction of CuNPs with bacterial cells because of F127 improves penetration through the membrane. All together, it could be because the nanoparticles had better copper ion migration, which killed the bacteria [46].

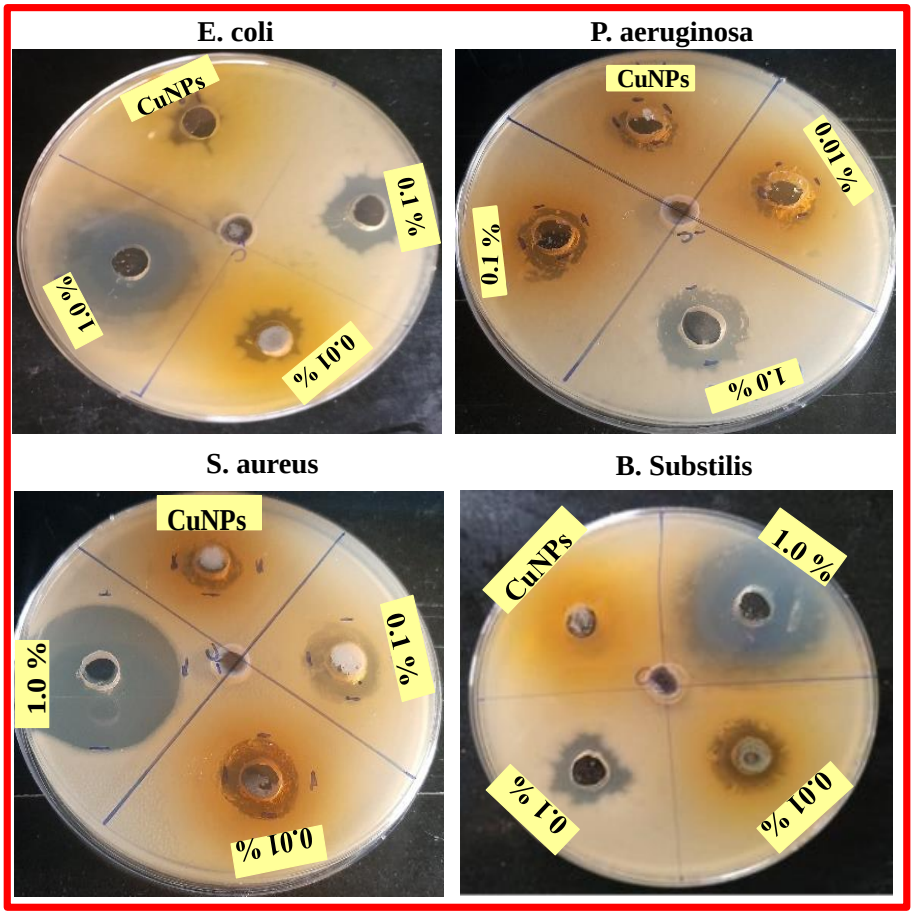

Figure 3.9: The images of the antibacterial activity of the blank and F127 mediated CuNPs against *E. coli* and *P. aeruginosa* as the Gram-negative bacteria and *S. aureus* and *B. subtilis* as the Gram-positive bacteria.

Table 3.3: Zones of inhibition analyses for F127 mediated CuNPs against Gram-negative and Gram-positive bacteria cells.

Test Sample	Zone of Inhibition (mm)			
	E. coli	***P. aeruginosa***	***S. aureus***	***B. subtilis***
Control	00	00	00	00
CuNPs	9 ± 0.8	6 ± 0.6	7 ± 0.4	8 ± 0.1
CuNPs in 0.01% F127	12 ± 0.5	8 ± 0.3	10 ± 0.6	11 ± 0.8
CuNPs in 0.1% F127	14 ± 0.6	9 ± 0.3	12 ± 0.9	12 ± 0.1
CuNPs in 1.0% F127	16 ± 0.6	11 ± 0.4	17 ± 0.8	16 ± 0.9

3.3.3.2: Antifungal activity

Figure 3.10 shows the zones of inhibition of *Penicillium*, *A. niger*, and *S. cerevisiae* fungi cells by using blank CuNPs and F127 mediated CuNPs. Inhibition growth showed an increase in all the fungus in the case of F127 mediated CuNPs. The growth of inhibition over *Penicillium*, *A. niger*, and *S. cerevisiae* and *F. oxysporum* dramatically increases with the rise in the concentration of F127 polymer and decrease in particle size (found in XRD results). As observed in the antibacterial studies, here too, the highest growth inhibition was found by the CuNPs prepared in the 1.0% F127 polymer (see Table 3.4).

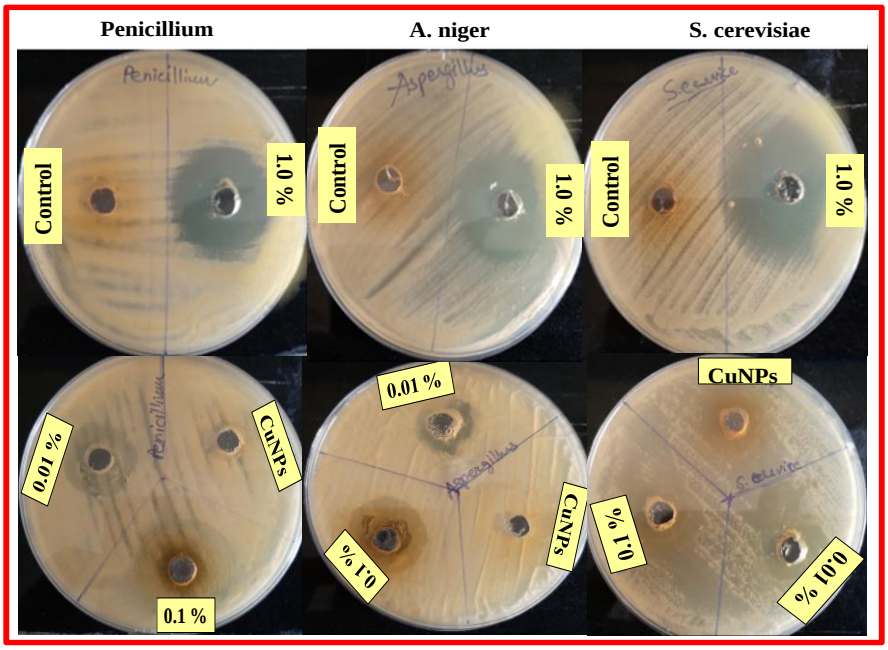

Figure 3.10: Antifungal activity of the blank and F127 mediated CuNPs against *Penicillium*, *A. niger*, and *S. cerevisiae* fungus.

Table 3.4: Zones of inhibition of F127 mediated CuNPs against selected funguses.

Test Sample	Zone of Inhibition (mm)		
	Penicillium	***A. niger***	***S. cerevisiae***
Control	00	00	00
CuNPs	5 ± 0.4	5 ± 0.9	7 ± 1.5
CuNPs in 0.01% F127	8 ± 0.6	7 ±2.3	10 ± 1.3
CuNPs in 0.1% F127	10 ± 0.4	9 ± 0.5	12 ± 0.5
CuNPs in 1.0% F127	23 ± 0.3	15 ± 1.3	23 ± 2.4

Not only that, we also evaluated the inhibitory activity against a representative *F. oxysporum* fungus versus time of treatment. Figure 3.11 provides the zones of inhibition of blank CuNPs and F127 mediated CuNPs samples over *F. oxysporum*. Table 3.5 presents data on the antifungal assays of CuNPs against *F. oxysporum* cells measured after 3 days, 5 days, and 7 days of treatment. The inhibitory effect of CuNPs on *F. oxysporum* growth increased with treatment incubation time. The highest growth inhibition was obtained in CuNPs with 1.0% F127 due to the smallest particle size of 38.12 nm.

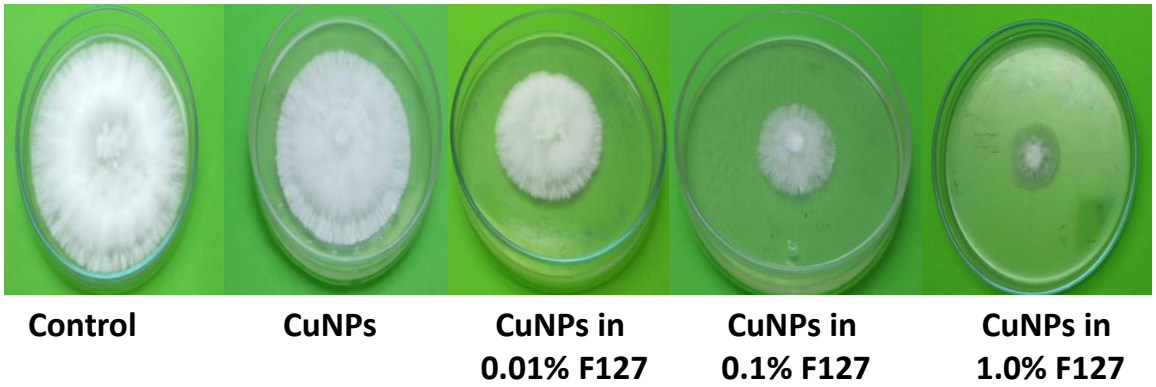

Figure 3.11: Growth inhibition of the blank and F127 mediated CuNPs against *F. oxysporum*.

Table 3.5: Inhibition growth of CuNPs against *F. oxysporum* fungus at different incubation time.

Test Sample	**Growth Inhibition (%)**		
	3 days	***5 days***	***7 days***
Control	64.6 ± 1.4 %	28.2 ± 1.8 %	0 ± 0.8 %
CuNPs	81.0 ± 1.6 %	61.2 ± 1.6 %	40.3 ± 1.7 %
CuNPs in 0.01% F127	92.4 ± 1.4%	82.3 ± 1.9%	72.2 ± 1.6 %
CuNPs in 0.1% F127	95.8 ± 1.6 %	86.6 ± 1.5 %	76.4 ± 1.5 %
CuNPs in 1.0% F127	98.2 ± 1.2 %	91.2 ± 1.7 %	84.3 ± 1.6 %

3.4: References

1. Baig, N., Kammakakam, I., Falath, W. and Kammakakam, I., 2021. Nanomaterials: a review of synthesis methods, properties, recent progress, and challenges. Mater Adv 2 (6): 1821–1871.
2. Ozin, G.A., 1992. Nanochemistry: synthesis in diminishing dimensions. *Advanced materials*, *4*(10), pp.612-649.
3. Mourdikoudis, S., Pallares, R.M. and Thanh, N.T., 2018. Characterization techniques for nanoparticles: comparison and complementarity upon studying nanoparticle properties. *Nanoscale*, *10*(27), pp.12871-12934.
4. Khan, I., Saeed, K. and Khan, I., 2019. Nanoparticles: Properties, applications and toxicities. *Arabian journal of chemistry*, *12*(7), pp.908-931.
5. Tanabe, K., 2007. Optical radiation efficiencies of metal nanoparticles for optoelectronic applications. *Materials Letters*, *61*(23-24), pp.4573-4575.
6. Zaera, F., 2013. Nanostructured materials for applications in heterogeneous catalysis. *Chemical Society Reviews*, *42*(7), pp.2746-2762.
7. Kim, Y.H., Kang, Y.S., Lee, W.J., Jo, B.G. and Jeong, J.H., 2006. Synthesis of Cu nanoparticles prepared by using thermal decomposition of Cu-oleate complex. *Molecular Crystals and Liquid Crystals*, *445*(1), pp.231-521.
8. Zhang, Q.L., Yang, Z.M., Ding, B.J., Lan, X.Z. and Guo, Y.J., 2010. Preparation of copper nanoparticles by chemical reduction method using potassium borohydride. *Transactions of Nonferrous Metals Society of China*, *20*, pp.s240-s244.
9. Liu, Q.M., Yasunami, T., Kuruda, K. and Okido, M., 2012. Preparation of Cu nanoparticles with ascorbic acid by aqueous solution reduction method. *Transactions of Nonferrous Metals Society of China*, *22*(9), pp.2198-2203.
10. Yang, J.G., Okamoto, T., Ichino, R., Bessho, T., Satake, S. and Okido, M., 2006. A simple way for preparing antioxidation nano-copper powders. *Chemistry Letters*, *35*(6), pp.648-649.
11. Siddiqui, M.A., Alhadlaq, H.A., Ahmad, J., Al-Khedhairy, A.A., Musarrat, J. and Ahamed, M., 2013. Copper oxide nanoparticles induced mitochondria mediated apoptosis in human hepatocarcinoma cells. *PloS one*, *8*(8), p.e69534.

12. Zhu, H., Zhang, C. and Yin, Y., 2005. Novel synthesis of copper nanoparticles: influence of the synthesis conditions on the particle size. *Nanotechnology*, *16*(12), p.3079.
13. Nakamura, T., Tsukahara, Y., Sakata, T., Mori, H., Kanbe, Y., Bessho, H. and Wada, Y., 2007. Preparation of monodispersed Cu nanoparticles by microwave-assisted alcohol reduction. *Bulletin of the Chemical Society of Japan*, *80*(1), pp.224-232.
14. Ahamed, M., Alhadlaq, H.A., Khan, M.M., Karuppiah, P. and Al-Dhabi, N.A., 2014. Synthesis, characterization, and antimicrobial activity of copper oxide nanoparticles. *Journal of Nanomaterials*, *2014*, pp.17-17.
15. Xiong, J., Wang, Y., Xue, Q. and Wu, X., 2011. Synthesis of highly stable dispersions of nanosized copper particles using L-ascorbic acid. *Green Chemistry*, *13*(4), pp.900-904.
16. Suárez-Cerda, J., Espinoza-Gómez, H., Alonso-Núñez, G., Rivero, I.A., Gochi-Ponce, Y. and Flores-López, L.Z., 2017. A green synthesis of copper nanoparticles using native cyclodextrins as stabilizing agents. *Journal of Saudi Chemical Society*, *21*(3), pp.341-348.
17. Kanhed, P., Birla, S., Gaikwad, S., Gade, A., Seabra, A.B., Rubilar, O., Duran, N. and Rai, M., 2014. In vitro antifungal efficacy of copper nanoparticles against selected crop pathogenic fungi. *Materials Letters*, *115*, pp.13-17.
18. Garg, J., Poudel, B., Chiesa, M., Gordon, J.B., Ma, J.J., Wang, J.B., Ren, Z.F., Kang, Y.T., Ohtani, H., Nanda, J. and McKinley, G.H., 2008. Enhanced thermal conductivity and viscosity of copper nanoparticles in ethylene glycol nanofluid. *Journal of Applied Physics*, *103*(7).
19. Umer, A., Naveed, S., Ramzan, N. and Rafique, M.S., 2012. Selection of a suitable method for the synthesis of copper nanoparticles. *Nano*, *7*(05), p.1230005.
20. Chidurala, S.C., Kalagadda, V.R. and Tambur, P., 2016. Antimicrobial activity of pure Cu nano particles synthesized by surfactant varied chemical reduction method. *Environmental Nanotechnology, Monitoring & Management*, *6*, pp.88-94.
21. Chatterjee, A.K., Chakraborty, R. and Basu, T., 2014. Mechanism of antibacterial activity of copper nanoparticles. *Nanotechnology*, *25*(13), p.135101.
22. Cao, V.D., Nguyen, P.P., Khuong, V.Q., Nguyen, C.K., Nguyen, X.C., Dang, C.H. and Tran, N.Q., 2014. Ultrafine copper nanoparticles exhibiting a powerful antifungal/killing

activity against Corticium salmonicolor. *Bulletin of the Korean Chemical Society*, *35*(9), pp.2645-2648.

23. Usman, M.S., Zowalaty, M.E.E., Shameli, K., Zainuddin, N., Salama, M. and Ibrahim, N.A., 2013. Synthesis, characterization, and antimicrobial properties of copper nanoparticles. *International journal of nanomedicine*, pp.4467-4479.
24. Ouda, S.M., 2014. Antifungal activity of silver and copper nanoparticles on two plant pathogens, Alternaria alternata and Botrytis cinerea. *Research Journal of Microbiology*, *9*(1), p.34.
25. Reverberi, A.P., Salerno, M., Lauciello, S. and Fabiano, B., 2016. Synthesis of copper nanoparticles in ethylene glycol by chemical reduction with vanadium (+ 2) salts. *Materials*, *9*(10), p.809.
26. Kumar, N. and Upadhyay, L.S.B., 2016. Facile and green synthesis of highly stable l-cysteine functionalized copper nanoparticles. *Applied Surface Science*, *385*, pp.225-233.
27. Tan, K.S. and Cheong, K.Y., 2013. Advances of Ag, Cu, and Ag–Cu alloy nanoparticles synthesized via chemical reduction route. *Journal of nanoparticle research*, *15*, pp.1-29.
28. Jana, N.R., Wang, Z.L., Sau, T.K. and Pal, T., 2000. Seed-mediated growth method to prepare cubic copper nanoparticles. *CURRENT SCIENCE-BANGALORE-*, *79*(9), pp.1367-1369.
29. Mott, D., Galkowski, J., Wang, L., Luo, J. and Zhong, C.J., 2007. Synthesis of size-controlled and shaped copper nanoparticles. *Langmuir*, *23*(10), pp.5740-5745.
30. Jeong, S., Woo, K., Kim, D., Lim, S., Kim, J.S., Shin, H., Xia, Y. and Moon, J., 2008. Controlling the thickness of the surface oxide layer on Cu nanoparticles for the fabrication of conductive structures by ink-jet printing. *Advanced functional materials*, *18*(5), pp.679-686.
31. Phul, R., Kaur, C., Farooq, U. and Ahmad, T., 2018. Ascorbic acid assisted synthesis, characterization and catalytic application of copper nanoparticles. *Material Science and Engineering International Journal*, *2*, pp.90-94.
32. Blanco-Andujar, C. and Thanh, N.T., 2010. Synthesis of nanoparticles for biomedical applications. *Annual Reports Section" A"(Inorganic Chemistry)*, *106*, pp.553-568.

33. Fusco, S., Borzacchiello, A. and Netti, P.A., 2006. Perspectives on: PEO-PPO-PEO triblock copolymers and their biomedical applications. *Journal of Bioactive and Compatible Polymers*, *21*(2), pp.149-164.
34. Pitto-Barry, A. and Barry, N.P., 2014. Pluronic® block-copolymers in medicine: from chemical and biological versatility to rationalisation and clinical advances. *Polymer Chemistry*, *5*(10), pp.3291-3297.
35. Desai, P.R., Jain, N.J., Sharma, R.K. and Bahadur, P., 2001. Effect of additives on the micellization of PEO/PPO/PEO block copolymer F127 in aqueous solution. *Colloids and Surfaces A: Physicochemical and Engineering Aspects*, *178*(1-3), pp.57-69.
36. Patel, H.S., Shaikh, S.J., Ray, D., Aswal, V.K., Vaidya, F., Pathak, C. and Sharma, R.K., 2022. Formulation, solubilization, and in vitro characterization of quercetin-incorporated mixed micelles of PEO-PPO-PEO block copolymers. *Applied Biochemistry and Biotechnology*, pp.1-19.
37. Singla, P., Garg, S., McClements, J., Jamieson, O., Peeters, M. and Mahajan, R.K., 2022. Advances in the therapeutic delivery and applications of functionalized Pluronics: A critical review. *Advances in Colloid and Interface Science*, *299*, p.102563.
38. Boca, S.C., Potara, M., Gabudean, A.M., Juhem, A., Baldeck, P.L. and Astilean, S., 2011. Chitosan-coated triangular silver nanoparticles as a novel class of biocompatible, highly effective photothermal transducers for in vitro cancer cell therapy. *Cancer letters*, *311*(2), pp.131-140.
39. Rahme, K., Gauffre, F., Marty, J.D., Payré, B. and Mingotaud, C., 2007. A systematic study of the stabilization in water of gold nanoparticles by poly (ethylene oxide)− poly (propylene oxide)− poly (ethylene oxide) triblock copolymers. *The Journal of Physical Chemistry C*, *111*(20), pp.7273-7279.
40. Sakai, T. and Alexandridis, P., 2004. Single-step synthesis and stabilization of metal nanoparticles in aqueous pluronic block copolymer solutions at ambient temperature. *Langmuir*, *20*(20), pp.8426-8430.
41. Rajesh, K.M., Ajitha, B., Reddy, Y.A.K., Suneetha, Y. and Reddy, P.S., 2016. Synthesis of copper nanoparticles and role of pH on particle size control. *Materials Today: Proceedings*, *3*(6), pp.1985-1991.

42. Zhou, T., Zhu, J., Gong, L., Nong, L. and Liu, J., 2019. Amphiphilic block copolymer-guided in situ fabrication of stable and highly controlled luminescent copper nanoassemblies. *Journal of the American Chemical Society*, *141*(7), pp.2852-2856.
43. Tokarek, K., Hueso, J.L., Kuśtrowski, P., Stochel, G. and Kyzioł, A., 2013. Green synthesis of chitosan-stabilized copper nanoparticles. *European Journal of Inorganic Chemistry*, *2013*(28), pp.4940-4947.
44. Kvítek, L., Panácek, A., Soukupová, J., Kolár, M. and Vecerová, R., 2008. R. P rucek, M. Holecová, R. Zboril. *J. Phys. Chem. C*, *112*, p.5825.
45. Zhang, G., Liu, J., Xu, Z., He, Y. and Kan, R., 2016. Characterization of temperature non-uniformity over a premixed CH 4–air flame based on line-of-sight TDLAS. *Applied Physics B*, *122*, pp.1-9.
46. Tamayo, L., Azócar, M., Kogan, M., Riveros, A. and Páez, M., 2016. Copper-polymer nanocomposites: An excellent and cost-effective biocide for use on antibacterial surfaces. *Materials Science and Engineering: C*, *69*, pp.1391-1409.